Article

Encapsulated Activated Grape Seed Extract: A Novel Formulation with Anti-Aging, Skin-Brightening, and Hydration Properties

Kan Tao [1], Lili Guo [1], Xincheng Hu [1], Corey Fitzgerald [2], Karl Rouzard [2], Jason Healy [2], Masanori Tamura [2], Jeffry B. Stock [2,3], Maxwell Stock [2], Eduardo Pérez [2] and José R. Fernández [2,*]

1   Research and Development Department, Shanghai Chicmax Cosmetic Co., Ltd., Floor 38, Global Harbor B, No 3300 North Zhongshan Road, Putuo District, Shanghai 200065, China; taokan@chicmax.net (K.T.); 60003145@kans.cn (L.G.); huxincheng@chicmax.net (X.H.)
2   Research and Development Department, Signum Biosciences, 11 Deer Park Drive Suite 202, Monmouth Junction, NJ 08852, USA; cwebb@signumbio.com (C.F.); krouzard@signumbio.com (K.R.); jhealy@signumbio.com (J.H.); mtamura@signumbio.com (M.T.); jstock@princeton.edu (J.B.S.); mstock@signumbio.com (M.S.); eperez@signumbio.com (E.P.)
3   Department of Molecular Biology, Princeton University, Princeton, NJ 08852, USA
*   Correspondence: jfernandez@signumbio.com; Tel.: +1-732-329-6344; Fax: +1-732-329-8344

Abstract: Protein phosphatase 2A (PP2A) is a master regulatory protein that plays a critical role in oxidative stress signaling. A novel, proprietary grape seed extract called Activated Grape Seed Extract (AGSE), enriched for PP2A-activating flavonoids, was recently developed and demonstrated to have antioxidant and anti-inflammatory activities. AGSE is a purple-colored powder, with limited solubility restricting its use in a broad range of formulations. Our aim was to develop a formulation that reduced the color and increased the solubility of AGSE, allowing its skin-health-enhancing properties to be utilized in a wider array of products, and to test it clinically. Encapsulation was performed utilizing a liposome and hydroxypropyl-β-cyclodextrin, (HPCD)-based approach to produce Encapsulated AGSE (E-AGSE). Human dermal fibroblasts and epidermal keratinocytes were used to determine expression levels of aging and dermal–epidermal junction (DEJ) markers. EpiDerm™ was UVB-irradiated to measure the effects against cytokine release, DNA damage, apoptosis, and skin barrier. Human melanocytes were used to determine melanin production and mushroom tyrosinase was used for inhibitory activity. A 4-week, 31-subject sensitive-skin clinical was performed with 2% E-AGSE Essence to assess its activity on human skin. We demonstrated that E-AGSE inhibits PP2A demethylation, increases key anti-aging (collagen I, III, elastin) and DEJ markers, protects against UVB-induced DNA damage, reduces inflammation, and promotes filaggrin in vitro. Moreover, E-AGSE reduces melanin production via tyrosinase inhibition. Clinical assessment of E-AGSE showed that it reduces the appearance of wrinkles, brightens the skin, and boosts hydration. E-AGSE is a novel grape seed extract formulation enriched for PP2A-activating flavonoids that is clinically effective in sensitive skin, providing several benefits.

Keywords: PP2A; grape seed; liposomes; hydroxypropyl-β-cyclodextrin; ultraviolet B

1. Introduction

Oxidative stress and ultraviolet (UV) light radiation are major detrimental factors in skin tone and aging [1,2]. Oxidative stress is provoked by the production and release of reactive oxygen species (ROS), which is amplified during dermal aging. Moreover, prolonged exposure to ultraviolet light A (UVA) and ultraviolet light B (UVB) triggers signaling cascades in dermal fibroblasts and keratinocytes, resulting in inflammation, melanin production, DNA damage, and photoaged skin [3,4]. An emerging target that plays a critical role in oxidative stress signaling, inflammation, skin barrier function, and

melanogenesis is Protein phosphatase 2A (PP2A). PP2A is a master regulator protein composed of three subunits: A (structural), C (catalytic), and B (regulatory). ROS have been shown to inactivate PP2A [5], resulting in activation of nuclear factor kappa B (NF-κB)-mediated pro-inflammatory signaling. In human dermal fibroblasts, oxidative stress drives the disassociation of the fully active PP2A holoenzyme trimer to the less active dimeric form [6]. PP2A activation has been proposed as a potential therapeutic target for combating oxidative stress [7] and is required for proper epidermal barrier formation during late embryonic development [8]. Additionally, a decrease in PP2A activity has been shown to lead to failures in filaggrin processing, which is essential for epidermal barrier homeostasis [9]. Moreover, ceramides, which play a critical role in skin barrier function, have been reported to activate PP2A [10], as has α-tocopherol (Vitamin E), a commonly used topical antioxidant [11]. Lastly, PP2A has been suggested to be involved in melanogenesis via proteasomal degradation of tyrosinase [12]. Altogether, these data suggest that maintaining PP2A in its active state is critical for combating oxidative stress and promoting healthier, brighter skin.

Vitis vinifera (grape) seed extracts are rich in bioactive polyphenols, such as flavonoids, that have been previously reported to possess strong anti-inflammatory, antioxidant, anti-aging, and skin-brightening properties [13–15]. Due to this broad range of activities, extracts rich in flavonoids are commonly used in cosmetic skincare products [16]. We recently reported the identification and characterization of activated grape seed extract (AGSE), a novel grape seed extract enriched with PP2A-activating flavonoids that has effective anti-aging activity and is significantly more potent than commercial grape seed extract in inhibiting PP2A demethylation [17]. In addition, our research demonstrates that AGSE blended with a novel fermentation product provides potent antioxidant protection by mitigating UV-induced photoaging and matrix metallopeptidase-1 (MMP-1) production to protect against skin aging [18]. However, AGSE is a dark, purple-colored powder, making it difficult to use in a broad range of topical formulations. Nanotechnology offers effective means to help mitigate a cosmetic ingredient's color by enhancing its activity and transdermal absorption [19]. With the rise in use of botanical extracts and their active ingredients in functional cosmetics, the importance and utilization of nanocarriers in skincare has also increased since their initial use over 35 years ago [20]. Encapsulation of a pigmented cosmetic ingredient into polymeric nanoparticles could enhance an ingredient's transdermal absorption profile, which would allow for preserved activity at lower concentrations and would thus decrease the color of the material used for topical formulation [21]. Moreover, nanocarriers offer several additional advantages such as higher solubility, improved stability, controlled release, reduced skin irritancy, color reduction of the formulation, and protection from degradation [20,22]. Considering the benefits of a nanocarrier, encapsulated AGSE (E-AGSE) was created using both liposomes and micelles via a hydroxypropyl-β-cyclodextrin (HPCD)-based approach, resulting in a more soluble, lighter-colored formulation that is more amenable to a wide range of uses in skincare products.

Here, we demonstrate for the first time that E-AGSE promotes the production of collagen I, collagen III, elastin, and dermal–epidermal junction markers critical for combating skin aging. We also show that E-AGSE not only protects the skin against UVB-induced inflammation, but also provides protection against UVB-induced DNA damage and can induce filaggrin production to help maintain a healthy skin barrier. E-AGSE's broad range of activity extends to melanocytes, in which it reduces melanin production and exhibits tyrosinase inhibitory activity. Lastly, clinical results in human subjects demonstrate 2% E-AGSE Essence is well tolerated and clinically effective, significantly reducing the appearance of wrinkles and promoting skin brightness and hydration when applied topically.

2. Materials and Methods

2.1. Reagents

All reagents were purchased from Sigma Chemical Co. (St. Louis, MO, USA). Organic solvents were purchased from Fisher Scientific (Hampton, NH, USA). Certificates of analysis were verified for all chemicals used to confirm > 95% purity. Butylene glycol was obtained from DAICEL (Tokyo, Japan). Hydroxypropyl-β-cylodextrin was obtained from Henan Yibo Biological Technology Co., Ltd. (Zhengzhou, China). Hydroxyacetophenone and 1,2-hexanediol were sourced from Symrise (Holzminden, Germany). Soybean lecithin was obtained from Tywei (Shanghai, China). Cholesterol was sourced from Cool Chemistry (Beijing, China).

2.2. AGSE and E-AGSE Production

AGSE was prepared as described in US patent no. 10,912,812 B2 [17]. The resulting AGSE material is a glassy, purple/black-colored solid. E-AGSE was prepared by adding 10 g AGSE powder to 50–75 g butylene glycol and stirring at room temperature for 18 h to dissolve (Phase A). Subsequently, 300 g HPCD was added to 200 g water and stirred at 90 °C until dissolved, and then cooled down to room temperature to obtain a transparent cyclodextrin solution (Phase B). Next, 5–10 g soybean lecithin and 1–2 g cholesterol were added into 25–50 g butylene glycol and mixed until dissolved at 70 °C (Phase C). Meanwhile, 5 g hydroxyacetophenone and 5 g 1,2-hexanediol were dissolved in water and sterilized, and then cooled down to room temperature for later use (Phase D). Phase B was added into Phase A, and the mixture stirred at room temperature for 12 h. The mixture was then added into Phase D and stirred for 4 h. The mixture of Phase A, Phase B, and Phase D was heated up to 70 °C, and then Phase C was added into the mixture and stirred at 70 °C for 5 to 10 minutes. After stirring, the mixture was cooled to 40 °C. Subsequently, the mixture was treated with high-pressure homogenization (HPH) using a UH-200 (Union-Biotech, Shanghai, China) to obtain 1 kg E-AGSE nanoparticles. Finally, particle size was analyzed using dynamic light scattering (DLS) (Mastersizer 2000, Malvern, Herrenberg, Germany).

2.3. PP2A Demethylation Assay

The [3H]-labeled methylated PP2A AC dimer was prepared by incubating PP2A, leucine carboxyl methyltransferase 1 (LCMT1), and [3H]-S-adenosyl-L-methionine (SAM) (PerkinElmer; Waltham, MA, USA) in 50 mM MOPS-Na (pH 7.2), 5 mM $MgCl_2$, and 1 mM dithiothreitol (DTT) at room temperature for 1 hour. Demethylation of PP2A by protein phosphatase methylesterase-1 (PME-1) was measured using the radioactive filter binding assay format. PME-1 (20 nM) was incubated for 15 minutes with extract or compound, and then 20 nM of [3H]-labeled methylated PP2A AC dimer was added. Reactions were run at room temperature for 30 minutes and then applied to a 96-well filter plate (Millipore Co.; Burlington, MA, USA) containing 30% TCA, from which proteins were precipitated and separated from the excess of [3H]-SAM by washing with 70% ethanol. The [3H]-incorporation was measured using a TopCount NXT scintillation counter (PerkinElmer; Waltham, MA, USA). IC_{50} values were generated from dose–response curves using a four-parameter logistic curve fit in SigmaPlot (Systat Software, Inc., San Jose, CA, USA). Full dose–response curves were run for actives tested to reach activity saturation.

2.4. Cell Culture and Viability

Primary human dermal fibroblasts (HDFBs) and normal human melanocytes (NHMCs) were obtained from the Cell Bank of Guangdong Biocell Biotechnology Co., Ltd. (Dongguan, China). Primary normal human epidermal keratinocytes (NHEKs) were purchased from Thermo-Fisher (Carlsbad, CA, USA). HDFBs were grown in Dulbecco's modified Eagle's medium (DMEM, Gibco, New York, NY, USA) containing 10% (v/v) new bovine serum (NBS, Hangzhou, China). NHMCs and NHEKs were grown in Medium 254 and EpiLife® medium (ThermoFisher, Carlsbad, CA, USA) supplemented with human melanocyte or keratinocyte growth supplements, respectively. Skin equivalent model EpiDerm™ was pur-

chased from MatTek Corp (Ashland, MA, USA) and acclimated for 24 h before treatments. Cells and tissues were incubated under standard conditions (37 °C; 5% CO_2). Maximum nontoxic concentrations of each material were determined (Figure S3) by reduction of tetrazolium dye MTT 3-(4,5-dimethylthiazol-2-yl)-2,5-diphenyltetrazolium bromide to formazan and monitoring by optical density at 490 nm. Results from the MTT assay determined the concentrations tested for each cell-based assay. For cell monolayers, all actives were diluted directly into culture medium and compared to untreated cells. For 3D skin model EpiDerm™, treatments were applied topically, and the vehicle used was E-vehicle, which comprised 90% propylene glycol and 10% encapsulation carrier without AGSE.

2.5. UVB-Induced Inflammation

EpiDerm™ tissues were pretreated topically for 4 h before UVB irradiation under standard culture conditions. Later, medium was removed, tissues were washed with phosphate-buffered saline (PBS), and tissues were irradiated with UVB at 200 mJ/cm^2 without test materials using FS-20/T-12 bulbs (280–340 nm). After UVB irradiation, tissues were treated and incubated for 24 h under standard culture conditions. After incubation, culture media supernatants were used to measure IL-8 levels using a Human ELISA kit (BD Biosciences; Franklin Lakes, NJ, USA).

2.6. Tissue Histology

EpiDerm™ tissues were washed with PBS and fixed in 10% neutral-buffered formalin. Tissues were sent to Mass Histology Services (Worcester, MA, USA) for paraffin embedding and mounting. Briefly, tissues were dehydrated in graded alcohols and xylene and embedded in paraffin blocks. Five-micron thick sections were obtained and mounted onto microscope slides. Hematoxylin–eosin (H&E) staining was performed to analyze sunburn cells (SBCs). Antigen retrieval was performed using citrate pH 6.0 or Tris/EDTA pH 9 buffer solutions. Tissue sections were incubated with anti-thymine dimer (CPDs, clone H3) or anti-filaggrin (clone EPR21892) purchased from AbCam PLC (Waltham, MA, USA). Chromogenic visualization was obtained after incubation with appropriate secondary antibody conjugated to horseradish peroxidase (HRP) and diaminobenzidine (DAB) substrate kit (AbCam). Positive cells were counted using a light microscope.

2.7. Aging Marker Expression

HDFBs were seeded at 40–60% cell confluency. Treatments were performed for 24 h using TGF-β1 (100 ng/mL) as a positive control. After incubation, total RNA was extracted using RNAiso Plus (TaKaRa, Beijing, China) and subjected to first-strand cDNA synthesis using a PrimeScript™ RT reagent kit (TaKaRa, China). Quantitative RT-PCR was performed using SYBR Green Real Time PCR Master Mix (TaKaRa, China) in a CFX96 detection system (Bio-Rad, Hercules, CA, USA). Collagen III expression (forward primer: 5′-ACCAGGAGCTAACGGTCTCA-3′; reverse primer: 5′-TCTGATCCAGGGTTTCCATC-3′) was calculated via 2-ΔΔCt method using actin as a housekeeping gene. For collagen I and elastin protein levels, cells were fixed for 30 minutes with 4% formaldehyde, blocked with normal goat serum for 30 minutes, and later incubated with anti-elastin (Abcam) or anti-collagen I (Proteintech, Wuhan, China) overnight at 4 °C. Chromogenic visualization was obtained after incubation with secondary anti-rabbit antibody conjugated to DyLight®-488 (AbCam). Cell nuclei were stained with Hoechst 33,258 at 10 µg/mL, and the representative images were obtained using a fluorescence microscope.

2.8. Dermal–Epidermal Junction (DEJ) Marker Expression

NHEKs were seeded at 40-60% cell confluency. Treatments were performed for 24 h using L-rhamnose (1%) and glycyl-l-histidyl-lysine-Cu2+ (GHK-Cu) as positive controls. After incubation, total RNA was extracted using RNAqueous (Ambion, Austin, TX, USA) and subjected to first-strand cDNA synthesis using an RNA-to-cDNA™ RT reagent kit (ThermoFisher, Carlsbad, CA, USA). Quantitative RT-PCR was performed using TaqMan® Real

time PCR Master Mix (ThermoFisher, Carlsbad, CA, USA), specific Taqman® probes (OCLN, Hs01049883_m1; SDC1, Hs00174579_m1; HSPG2, Hs00194179_m1; CD44, Hs01075862_m1; GAPDH, Hs02786624_g1), and StepOnePlus™ (Applied Biosystems, Whaltman, MA, USA). Gene expression was calculated via $2^{-\Delta\Delta Ct}$ method using GAPDH as a housekeeping gene.

2.9. Melanin Assay

NHMC were seeded in 6-well plates at 2.2×10^5 cells/well and incubated for 24 h before treatments. Later, cells were treated for 72 h, washed twice with PBS, harvested, and lysed with 1 M NaOH for 30 min at 80 °C. Each suspension was centrifuged for 10 minutes at 10,000 rpm. Supernatants were obtained to measure melanin concentrations using synthetic melanin standard and an optical density of 405 nm.

2.10. Tyrosinase Assay

Mushroom tyrosinase (Sigma-Aldrich Co., St. Louis, MO, USA) was used to measure inhibition rate activity in sample dilutions. Test and control (Arbutin) samples were pre-incubated with the reaction mix system using L-dihydroxyphenylalanine (L-DOPA) as a substrate at 37 °C for 5 minutes. Tyrosinase enzyme was added, and the reaction performed at 37 °C for 10 minutes. Enzyme activity was monitored by dopachrome formation at 475 nm and inhibition activity was compared to vehicle-only control sample. E-AGSE was tested up to 10% to produce a full dose–response curve that reached 50% inhibition.

2.11. Clinical Study

A cosmetic clinical trial in healthy volunteers was conducted by a third-party contract research organization (SGS Stephens, Shanghai, China) with SGS job no. SHCPCH210201806. The study started on 26 February 2021 and was completed on 26 March 2021. A total of 31 Asian females with sensitive skin, ranging in age from 28 to 50 years, were enrolled. The study was conducted according to the guidelines of the Declaration of Helsinki and approved by the Institutional Review Board of SGS Stephens (No. SHCPCH210201806 and approved in January 2021). Subjects reported to the testing facility for baseline screening, at which time informed consent and demographics were obtained (Table S1 for subject demographics). Inclusion/exclusion criteria were verified using expert clinical grading evaluations to determine eligibility with the following conditions: sensitive skin type (score > 5 determined by lactic acid skin test), exhibiting skin redness (clinical score of skin redness > 2) according to SGS scales, skin hydration value less than 60 C.U.; skin transepidermal water loss (TEWL) value greater than 15 g/h/m^2; with no obvious skin lesions or scars on the test area. Lactic acid skin test was conducted by a technician by applying 10% lactic acid and water on the nose and grading the cutaneous reaction at various timepoints. Grading ranged from 0–3, where 0 = no reaction; 1 = slight stabbing pain, itching, and redness; 2 = moderate, can endure; and 3 = serious, cannot endure. Scores were then totaled, and a subtotal of >5 was classified as a sensitive skin type. Subjects received 2% E-AGSE Essence formulation (containing 0.02% AGSE), and were instructed to apply it morning and evening, and to use no other skincare products on their faces beginning one week prior to and continuing through the duration of the study. Study duration was 4 weeks with three evaluations: enrollment (baseline), week 2, and week 4. At each visit, subjects underwent several tests: skin tone (measured by Colorimeter® CL400 (Courage + Khazaka Electronic, Köln, Germany)), TEWL (measured by Tewameter® TM300 (Courage + Khazaka Electronic, Köln, Germany)), skin hydration (measured by Corneometer® CM825 (Courage + Khazaka Electronic, Köln, Germany)), lactic acid skin test (using 10% lactic acid/water on the nose), and a self-assessment questionnaire (evaluation criteria and results listed in Table 6). Photography and skin wrinkle area analysis were performed with VISIA CR.

2.12. Statistical Anlysis

Statistical significance for in vitro assays was determined by ANOVA followed by a Dunnett multiple-comparisons test using p-values less than 0.05 as a significant difference.

Concentration–response curves were generated by fitting data with the Hill three-parameter equation using the Sigma Plot software, from which the IC_{50} and maximum inhibition were determined. For clinical data, statistical significance was determined by *t*-test method using a two-tailed test, with p-values less than 0.05 considered to be a significant difference.

3. Results

3.1. Chemical Encapsulation of AGSE does Not Alter PP2A Activity

We previously demonstrated that AGSE contains a higher concentration of PP2A-activating flavonoids compared to commercially available grape seed extract and is thus ~5 times more potent for inhibiting PP2A demethylation [17]. Despite its broad array of antioxidant and anti-inflammatory properties which protect the skin against several different environmental stimuli, AGSE, like most commercial grape seed extracts, possesses a dark purple color and has poor solubility in aqueous formulations, which limits its use in consumer skincare products. To reduce its color during formulation development, but still increase its solubility and potentially enhance skin penetration, AGSE was encapsulated in two ways: (1) via liposomes and (2) via HPCD used as complexing agent (Figure 1A). Encapsulation of AGSE markedly improved both color and solubility when compared to AGSE formulated alone at the same solid content concentration (Figure 2). Color improvement was also quantitated by measuring absorbance at 480 nm, which further demonstrated that E-AGSE is lighter than AGSE with readings at 0.1478 and 0.3894, respectively. To determine stability, the particle size of the E-AGSE nanocarriers was measured by dynamic light scattering (DLS). The DLS experiment under aqueous solution indicated the nanocarrier had an average hydrodynamic diameter of 89 nm (Figure 1B). For cosmetic storage stability testing, the standard conditions measured to determine stability were after three months at 4 °C, room temperature, and 48 °C. To verify the stability of E-AGSE, particle size was measured after three months under those conditions, with additional tests performed at −18 °C, 48 °C, and with lighting for additional reference. Results showed that the particle size of E-AGSE was within stable range under all conditions tested (Table 1). Most notably, E-AGSE particle size remained stable at 48 °C, which is the most stringent industry standard for particle size stability. Lastly, the color appearance of E-AGSE also remained stable after 3 months under all conditions tested (Figure S1).

Table 1. E-AGSE particle size under different conditions.

Condition Group	Particle Size (Week 4)	Uniformity	Particle Size (Week 12)	Uniformity
room temperature	93 nm	0.314	94 nm	0.326
4 °C	95 nm	0.336	91 nm	0.316
−18 °C	82 nm	0.396	93 nm	0.325
48 °C	96 nm	0.369	119 nm	0.367
lighting	89 nm	0.301	93 nm	0.304

Data represent the average of three measurements.

Given PP2A's key role in oxidative stress, barrier repair, and inflammation, we wanted to ensure that E-AGSE retained its ability to keep PP2A in its more active, methylated, heterotrimeric form. Results showed that E-AGSE retained a similar effect of PP2A demethylation inhibition activity compared to nonencapsulated AGSE, with an IC_{50} of 0.0450 μg/mL and 0.0624 μg/mL, respectively (Figure 1C). This retention of activity demonstrates that encapsulation maintains AGSE activity and stability. Moreover, E-vehicle (encapsulation carrier without AGSE) was shown to not provide PP2A demethylation inhibition activity ($IC_{50} > 60$ μg/mL). Given these results and that the E-AGSE formulation contained only 1% AGSE, it is speculated that the nanocarriers may increase the potency of AGSE for inhibiting PP2A demethylation.
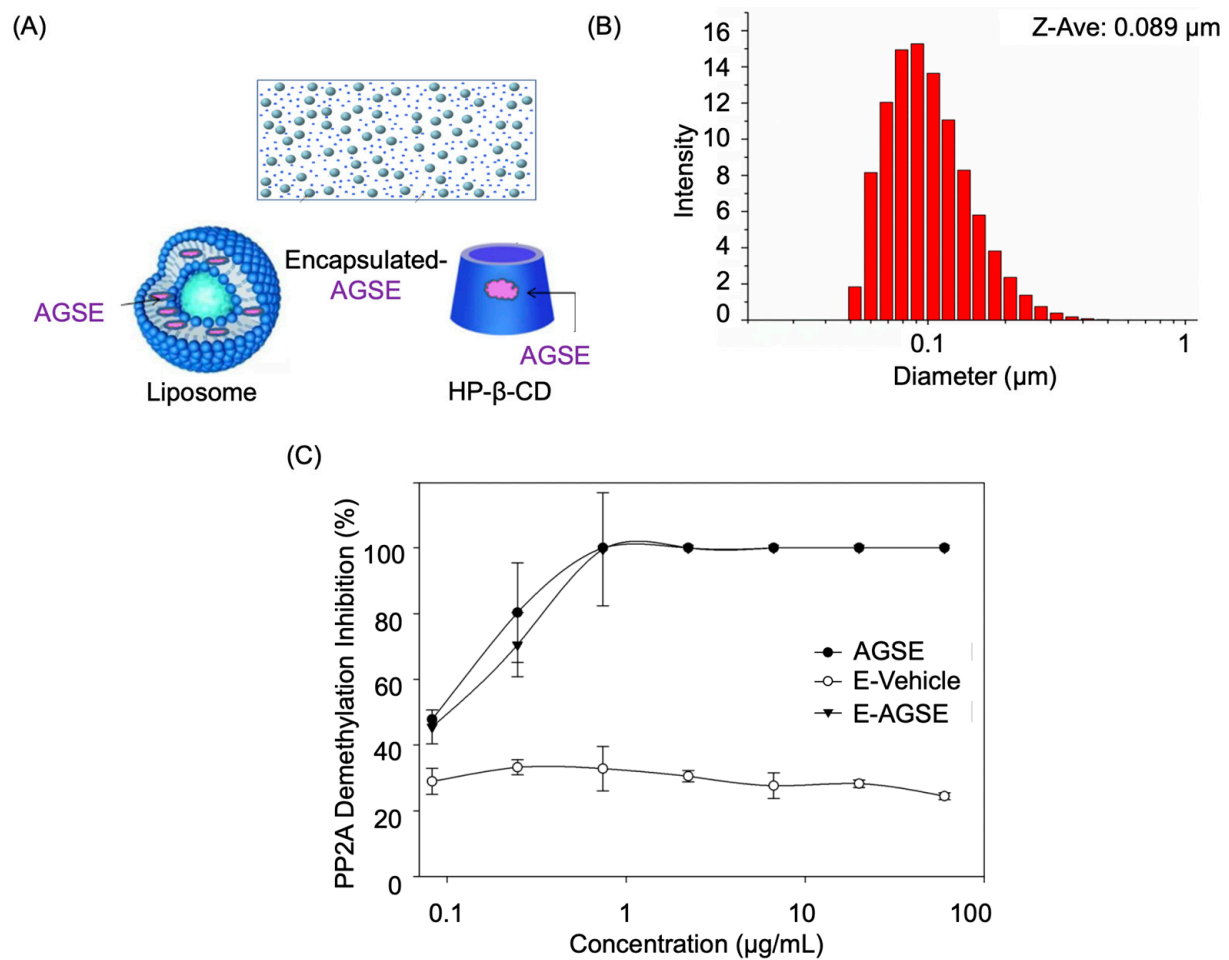
Figure 1. Chemical encapsulation of AGSE retains inhibition of PP2A demethylation activity. (**A**) Chemical encapsulation formulation utilizing liposome and HPCD-based approaches. (**B**) The particle size of the E-AGSE nanocarriers was measured by DLS. (**C**) The PP2A-demethylating enzyme PME1 and 3H methyl-tagged PP2A were incubated with various concentrations of AGSE and E-AGSE. Dose-dependent inhibition was monitored by 3H retained on methylated PP2A. The data represent the cumulative average ± SD of three independent experiments.
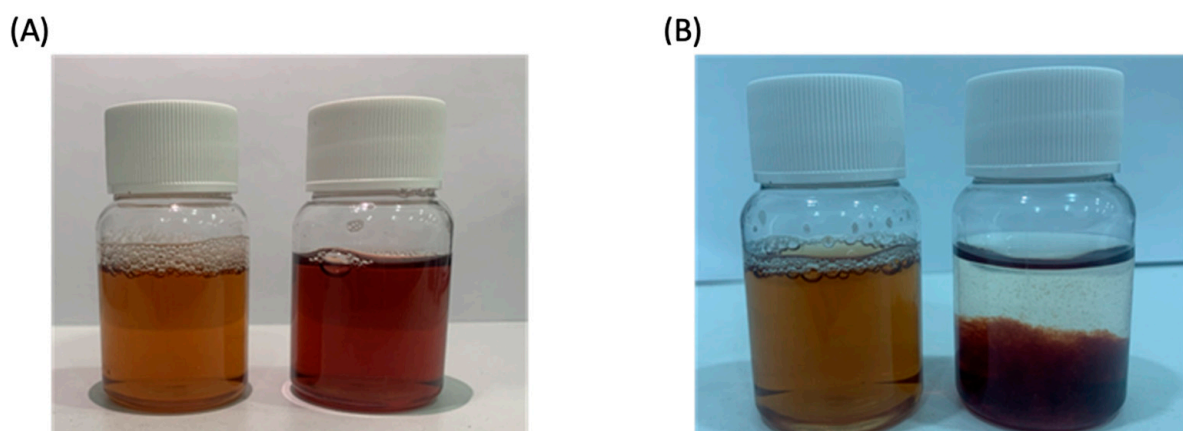

Figure 2. Chemical encapsulation of AGSE improves color and solubility. Comparison of 0.2% AGSE propylene glycol solution (left) and 2% E-AGSE (right) after (**A**) initial mixing and (**B**) 24 h.

3.2. E-AGSE Upregulates the Expression of Key Anti-Aging Extracellular Matrix Markers

Given the similar potency for PP2A activity displayed by AGSE and E-AGSE, we sought to characterize the potential additional benefits of E-AGSE on key skin targets located in the extracellular matrix (ECM). Collagens are essential scaffold proteins that promote skin firmness and mechanical resiliency, but their expression levels (Collagen types I and III) decline with age [23]. Moreover, elastin (ELN) has been shown to play a critical role in maintaining skin elasticity [24]. Utilizing human dermal fibroblasts (HDFs), cells were treated for 24 h, and total RNA was isolated to measure collagen III gene expression using quantitative PCR (qPCR). Collagen I and elastin protein levels were measured via immunofluorescence and the results are shown in Table 2. The results demonstrated that E-AGSE (0.1%) significantly increased collagen I (232%), collagen III (102%), and elastin (131%). In contrast, treatments with palmitoyl tripeptide-5 (8 ppm), a collagen-boosting ingredient commonly used in skincare products [25], produced a significant increase in collagen I (196%), but did not produce a significant increase in collagen III (58%) and had no effect on elastin expression (0%). Transforming growth factor beta-1 (TGF-β1) (100 ng/mL) was used as a positive control and increased collagen I (132%) and collagen III (89%) as expected.

Table 2. Results for anti-aging extracellular matrix marker expression.

Test Group	Avg ± SD (% Change from Untreated)		
	Immunofluorescence, IOD/Cell		Gene (Fold Expression)
	Collagen I *	Elastin *	Collagen III (COL3A1) ¥
Untreated	1.00 ± 0.05	1.00 ± 0.1	1.02 ± 0.28
TGF-β1 (100 ng/mL)	2.32 ± 0.21 (132%) **	ND	1.93 ± 0.08 (89%) **
E-AGSE (0.1%)	3.32 ± 0.28 (232%) **	2.31 ± 0.32 (131%) **	2.07 ± 0.10 (102%) **
Palmitoyl Tripeptide-5 (8 ppm)	2.96 ± 0.73 (196%) **	0.99 ± 0.21 (0%)	1.62 ± 0.41 (58%)

The data represent the average ± SD of cumulative data from three independent experiments. ** $p \leq 0.01$ indicates a statistically significant difference compared to untreated cells. * Measured via immunofluorescence using IOD (integral optical density) per cell. ¥ Measured via qPCR, normalized to level of actin as control housekeeping gene. ND = not determined.

3.3. E-AGSE Upregulates Dermal–Epidermal Junction (DEJ) Marker Expression

The skin aging process changes dermal–epidermal junctions (DEJ), resulting in a significant decrease in thickness and ECM markers [26]. Basal keratinocytes adjoin the DEJ surface, providing both structural support and space for molecular interaction with dermal fibroblasts [27]. Epidermal heparan sulphate proteoglycans (HS-PGs) and glycosaminoglycans (GAGs) are essential ECM components at the DEJ that provide structural orientation to other ECM constituents for molecular interaction [28]. Occludin (OCLN) is a specific marker for cell tight junctions [29], and syndecan-1 (SDC1), heparan sulfate proteoglycan 2 (HSPG2), and chondroitin sulfate proteoglycan 8 (CD44) have previously been shown to be decreased in atrophic skin [30]. We studied the effect of E-AGSE on the gene expression of both DEJ and GAGs by epidermal keratinocytes in culture. Utilizing human epidermal keratinocytes (NHEKs), cells were treated for 24 h, and total RNA was isolated to measure OCLN, SDC1, HSPG2, and CD44 gene expression levels using qPCR. The results demonstrated that E-AGSE (0.1%) significantly increased OCLN (885%), SDC1 (103%), HSPG2 (39%), and CD44 (47%) (Table 3). Gene expression activity associated with E-AGSE was higher than those associated with L-rhamnose [31] and tripeptide-copper complex glycyl-l-histidyl-lysine-Cu2+ (GHK-Cu) [32], used as positive controls for papillary dermis and glycosaminoglycan-boosting ingredients in skincare products, respectively (Table 3).

Table 3. Results for marker expression.

Test Group	Avg ± SD (% Change from Untreated) Gene (Fold Expression)			
	Occludin (OCLN) [¥]	Syndecan-1 (SDC1) [¥]	Heparan Sulfate Proteoglycan 2 (HSPG2) [¥]	Chondroitin Sulfate Proteoglycan 8 (CD44) [¥]
Untreated	1.00 ± 0.03	1.00 ± 0.02	1.00 ± 0.01	1.00 ± 0.02
L-Rhamnose (1%)	2.59 ± 1.27 (159%) **	1.41 ± 0.15 (41%) **	1.20 ± 0.21 (20%) *	1.20 ± 0.09 (20%) **
E-AGSE (0.1%)	9.85 ± 3.87 (885%) **	2.03 ± 0.37 (103%) **	1.39 ± 0.22 (39%) **	1.47 ± 0.21 (47%) **
GHK-Cu (0.05%)	1.99 ± 0.81 (99%) **	1.42 ± 0.22 (42%) **	1.21 ± 0.14 (21%) **	1.15 ± 0.04 (15%) **

The data represent the average ± SD of cumulative data from three independent experiments. * $p < 0.05$; ** $p \leq 0.01$ indicates a statistically significant difference compared to untreated cells. [¥] Measured via qPCR, normalized to level of GAPDH as control housekeeping gene.

3.4. E-AGSE Protects against UVB-induced DNA Damage and Promotes Epidermal Integrity

Ultraviolet light B (UVB)-induced skin inflammation is mediated via activation of the NFκB pathway, resulting in the release of several pro-inflammatory cytokines [33]. Given that polyphenols are reported to possess potent anti-inflammatory properties [15], we wanted to explore E-AGSE's anti-inflammatory activity using a 3D human skin model (EpiDerm™) irradiated with UVB. Tissues were topically pretreated with 10% E-AGSE (containing 0.1% AGSE) and the results demonstrated strong anti-inflammatory activity with E-AGSE significantly decreasing pro-inflammatory cytokine IL-8 production. While UVB + vehicle produced higher IL-8 levels compared to UVB-only, E-AGSE completely abrogated this effect, decreasing IL-8 by ~100% (Table 4). Filaggrin expression in skin has been linked with barrier function and UV sensitivity [34]. As shown in Figure 3, UVB irradiation produced a significant reduction in filaggrin expression, compromising the integrity of the epidermal barrier. Interestingly, E-AGSE applied topically to 3D skin exhibited a protective skin barrier effect, blocking the reduction of filaggrin levels after UVB exposure. Conversely, the encapsulation vehicle offered no protection, highlighting the effectiveness of AGSE.

Table 4. Results for UVB-induced skin damage in EpiDerm™.

Test Group	Avg ± SD (% Inhibition from UVB + Vehicle)		
	IL-8, pg/mL	CPDs (+Cells/Tissue) *	SBCs (+Cells/Tissue) *
Vehicle	220 ± 24	0 ± 1	6 ± 1
E-AGSE (0.1%)	121 ± 6	1 ± 2	1 ± 0
UVB (200 mJ/cm^2)	1051 ± 108	223 ± 1	24 ± 7
UVB + Vehicle	11321 ± 1850 (0 [#])	177 ± 33 (21% [#])	18 ± 3 (39% [#])
UVB + E-AGSE (0.1%)	339 ± 70 (98%) [‡]	86 ± 21 (52%) [‡]	7 ± 2 (93%) [‡]

The data represent the average ± SD from n = 3 tissues. * Positive cells were counted using a light microscope. [#] % inhibition calculated from UVB only. [‡] $p < 0.05$ indicates a statistically significant difference compared to UVB + Vehicle group.

To continue to explore the potential protective benefits against UVB, we next attempted to determine whether E-AGSE could protect against DNA damage. Two common markers for measuring UVB-induced damage are cyclobutene pyrimidine dimers (CPDs) and sunburn cells (SBCs) [35,36]. Our results show that skin treated with E-AGSE significantly inhibited the presence of CPDs formation by 52% as compared to only 21% by the vehicle control (Figure 3 + Table 4). Moreover, E-AGSE strongly inhibited SBC formation by 93%, while the vehicle control only conferred 39% protection (Figure 3 and Table 4).
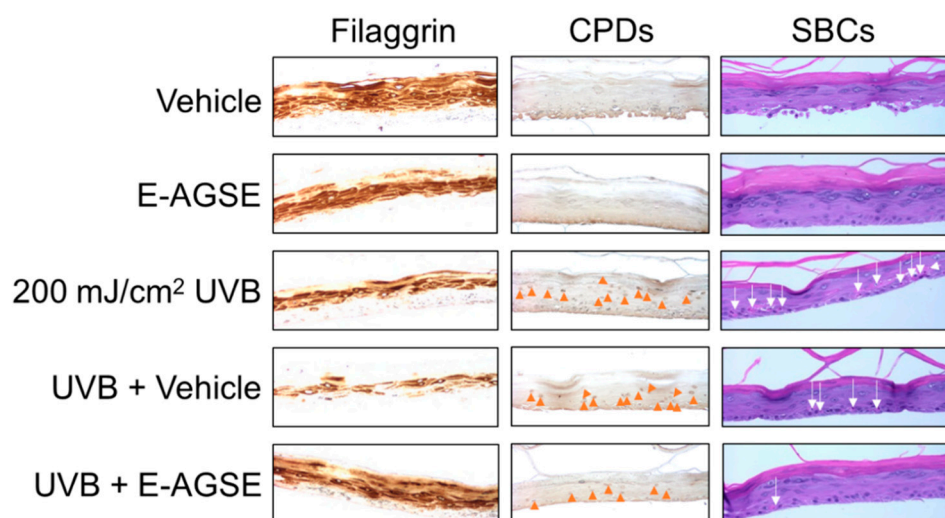
Figure 3. E-AGSE increases skin barrier components and protects from DNA damage after UVB irradiation. EpiDerm™ 3D skin culture models were topically pretreated with E-AGSE (0.1%) for 4 h, then irradiated with 200 mJ/cm^2 UVB and later incubated for 24 h with actives. Tissues were fixed in 10% formalin, paraffin embedded, and mounted on slides. Immunohistochemical staining (DAB) for filaggrin. Immunohistochemical staining (DAB) for CPDs and H&E staining for SBCs. Blue and white arrowheads indicate positive CPD and sunburn cells, respectively. Original magnification: ×200.

3.5. E-AGSE Demonstrates Skin-Brightening Properties

Oral intake of polyphenol-rich grape seed extract has previously been shown to provide skin-brightening effects via inhibition of melanin synthesis by tyrosinase [14], and a specific black grape seed extract, also rich in polyphenols, was shown to possess skin-brightening activity when used topically [37]. Thus, we wanted to determine whether E-AGSE could improve skin tone when applied to skin. Utilizing native human melanocytes (NHMCs), cells were treated for 72 h, and total melanin was extracted to measure the effect on melanin production. The results showed that 3-o-ethyl ascorbic acid (125 µg/mL) (a known skin-brightening agent) and E-AGSE (0.02%) significantly reduced melanin production in human melanocytes (Figure 4A). Tyrosinase is the first and rate-limiting step for melanin biosynthesis in melanocytes [38]. Assaying for tyrosinase enzymatic activity in the presence of E-AGSE and arbutin (a cosmetic skin-brightening agent), demonstrates that E-AGSE significantly and dose-dependently decreased the activity of tyrosinase (Figure 4B), as did arbutin (Figure S2).

3.6. E-AGSE Improves Skin Aging, Brightening, and Hydration in Human Subjects

Since E-AGSE demonstrated both anti-aging and skin-brightening activity in vitro, we sought to determine whether it could provide similar benefits when applied topically to human skin. Therefore, we performed a proof-of-concept clinical study via a third-party dermatology contract research organization (SGS Stephens Shanghai). This clinical study was conducted with 31 healthy female subjects to evaluate the potential anti-aging, skin-brightening, and hydrating properties of E-AGSE. E-AGSE was first tested clinically in a 24-hour human patch test and was found to cause no skin sensitization, irritation, or erythema (reference standard: GB17149.1-1997/GB17149.2-1997; data not shown). The clinical dose of 2% E-AGSE Essence, which contains 0.02% AGSE, was chosen because the suggested dosage for AGSE is 0.01–0.05% and the encapsulation rate for AGSE is 1%. 2% E-AGSE Essence was applied twice daily for 28 days. Image analysis of photos captured by VISIA CR demonstrated that 14 days after application, the appearance of wrinkles significantly decreased by 12% as compared to baseline, and this continued to improve at 4 weeks, reaching 13% reduction (Figure 5 and Table 5). To determine E-AGSE's potential skin-brightening properties, a Colorimeter® CL400 was utilized where the higher the skin

tone L* value, the brighter the skin. The results showed that after 2 weeks of application, subjects' skin tone was significantly brighter (5% improvement) when compared to baseline and was up to ~9% brighter after 4 weeks (Table 5). Skin hydration was measured using a Corneometer® and skin barrier function via trans epidermal water loss (TEWL) using a Tewameter®. The results demonstrated that E-AGSE produced statistically significant higher mean Corneometer® values when compared to baseline at 14 and 28 days, improving skin hydration by 25% and 31%, respectively (Table 5). Moreover, when compared to baseline, E-AGSE produced statistically significantly lower TEWL values at weeks 2 and 4, indicating an increase in skin barrier function (Table 5). Results from the lactic acid sting test showed significant improvement in sensitive skin type, with scores decreasing by 11.59% and 19.81% at week 2 and week 4, respectively (Table 5). Self-perception questionnaires (SPQs) completed by the subjects showed that after 28 days, 100% of the subjects reported improved skin elasticity, skin comfort, and hydration (Table 6). Moreover, >94% of subjects felt that their skin was brighter, firmer, and had a strengthened barrier and improvement in fine lines, all supporting the quantitative data that were measured in this study. Altogether, these results indicate that E-AGSE when topically applied reduces the appearance of wrinkles, brightens skin, boosts skin hydration and barrier function, and improves the condition of sensitive skin.
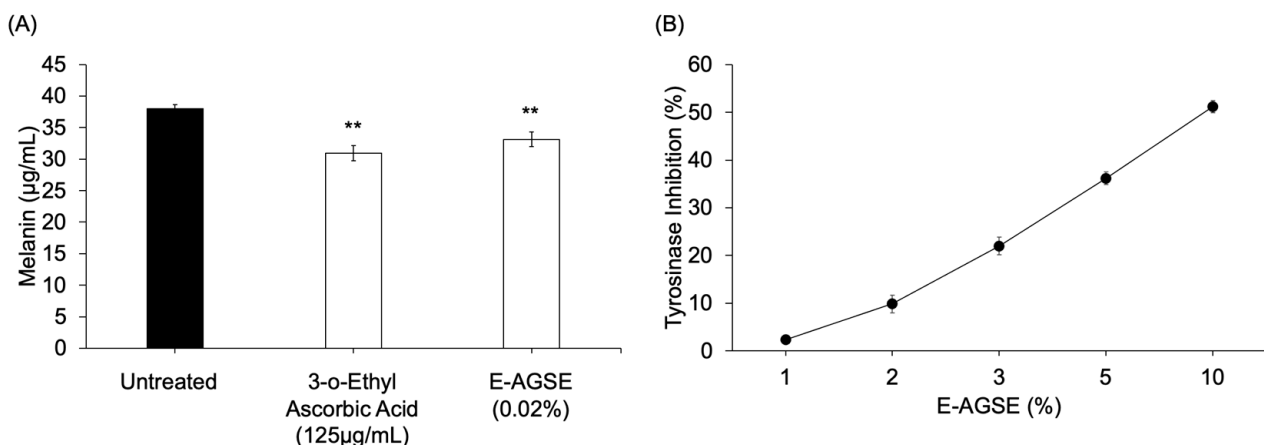

Figure 4. E-AGSE reduces melanin production and inhibits tyrosinase enzyme activity. (**A**) Normal human melanocytes (NHMCs) were treated with the indicated concentrations for 72 h and harvested for melanin content evaluation. The level of melanin was quantitated by colorimetric assay. The data represent the average $\pm$ SD of cumulative from three independent experiments. ** $p \leq 0.01$ indicates a statistically significant difference compared to untreated cells. (**B**) Mushroom tyrosinase enzymatic activity was evaluated using L-DOPA substrate and activity was monitored by dopachrome formation via optical density (475 nm). The data represent the average $\pm$ SD of cumulative from three independent experiments.
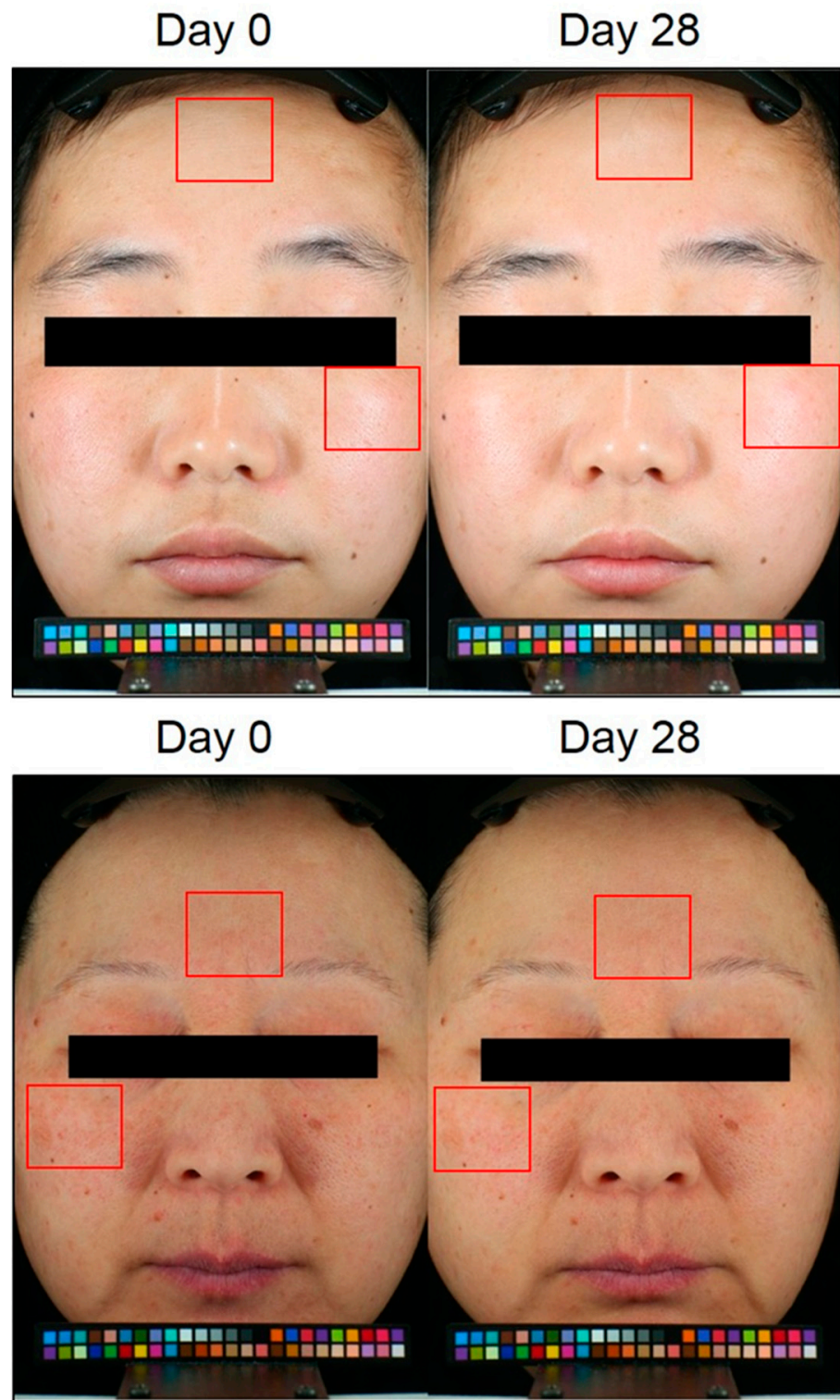
Figure 5. Clinical study utilizing E-AGSE showed improvement in anti-aging, hydration, and brightening endpoints. Standardized photographs of the face were taken at baseline and after 4 weeks of application. Skin wrinkles were analyzed using a VISIA®-CR Imaging system. Red boxes indicate areas of visible improvement in skin wrinkles (fine lines) and brightening. Skin moisture, TEWL, and color parameters were measured using Tewameter® and colorimeter instruments.

Table 5. Summary of clinical endpoints *.

Parameter (Instrument)	Time Point	Mean Change (Mean Change %) *	*p* Value **
Skin wrinkle area (VISIA CR)	Week 2	−11.20	<0.05
	Week 4	−13.66	<0.05
Skin tone/brightening (Colorimeter® CL400)	Week 2	+5.16	<0.05
	Week 4	+8.86	<0.05
TEWL (Tewameter® TM300)	Week 2	−7.15	<0.05
	Week 4	-10.10	<0.05
Skin hydration (Corneometer® CM825)	Week 2	+24.57	<0.05
	Week 4	+30.94	<0.05
Lactic acid sting test	Week 2	−11.59	<0.05
	Week 4	−19.81	<0.001

* Percent of the population that showed an improvement, calculated based on average rate of change. ** Calculated with *t*-test method using two-tailed test. Testing hypothesis was that the mean change from baseline was zero.

Table 6. Summary of SPQ endpoints for subjects applying 2% E-AGSE Essence.

Self-Perception Questionnaire (SPQ) Parameter	Week 2	Week 4
Improved skin elasticity	94%	100%
Improved skin comfort	100%	100%
Improved skin brightness	90%	94%
Improved skin hydration	97%	100%
Improved skin firmness	94%	94%
Skin feels hydrated and brightened	87%	90%
Improved fine lines/nasolabial folds	94%	94%
Improved dry and fragile skin	97%	97%
Soothed skin tightness	97%	94%
Soothed facial redness	90%	94%
Alleviated dryness and sensitivity	100%	97%
Repaired/strengthened the skin barrier	97%	97%
Skin quality improvement	100%	90%
Mild and not irritating	97%	100%

Evaluation criteria: Score (1 = disagree completely, 2 = disagree relatively, 3 = somewhat disagree, 4 = neither disagree nor agree, 5 = somewhat agree, 6 = agree relatively, 7 = agree completely). Satisfaction = number of subjects with score > 4 / total subjects × 100%.

4. Discussion

Since their discovery in grape seeds in 1947 [13], proanthocyanidins have been reported to provide several benefits to the skin, making grape seed extracts (GSEs) an attractive botanical source for use in the cosmetic industry. Despite GSEs' strong antioxidant, anti-inflammatory, and anti-aging properties, their formulation for topical use presents several challenges. First, GSEs rich in flavonoids tend to be poorly soluble in water, causing precipitation in aqueous formulations. Secondly, GSEs tend to have a dark purple and/or black color, hindering their use in light-colored topical formulations. To this end, GSEs are commonly formulated in emulsions consisting of two immiscible phases (an oil and a water phase), which helps to solubilize the flavonoids [39]. However, these two-phase emulsions can affect the stability and viscosity of polyphenol-rich topical formulations [16]. To help address these issues, we demonstrate here, utilizing nanotechnology, the successful development of a four-phase formulation that encapsulates activated grape seed extract (AGSE). The resulting E-AGSE possesses an improved solubility profile and lighter color

(Figure 2), with retained activity for skin and potential application in a broader range of cosmetic formulations.

Despite GSE's multifunctional activities in skin, little has been published to date on the activity of GSE when applied topically to human skin. We hypothesize that the difficulties in formulating GSE into topical formulations has contributed to this lack of study. As of this writing, search results displayed only two articles testing GSE in a topical formulation. Results from the first study demonstrated that a 2% GSE cream was effective in wound healing [40], while the other publication reported that a 2% black GSE in a water-in-oil emulsion applied to the face improved hyperpigmentation and skin elasticity [37]. Additional literature hints at the potential for utilizing GSE to combat damage caused to the skin by air pollution, but this topical formulation also contained green tea and oak wood extracts, making it difficult to discern which active and/or extract was responsible for the observed protective effect [41]. Similar findings have been published for GSE promoting hydration [42] and protecting against infrared-A damage [43], but once again, in both instances, GSE was combined with almost two dozen additional ingredients.

Here, we demonstrate for the first time that E-AGSE when applied topically provides the skin with several benefits, including reduced appearance of wrinkles, skin-brightening, and improved skin barrier function (Figure 5 and Table 5). These clinical findings confirm the wide range of in vitro activities reported here for E-AGSE. For example, we showed that E-AGSE promotes elastin and collagen I + III production (Table 2) which in part could explain the anti-aging benefits observed when applied topically. Moreover, our discovery that E-AGSE decreases melanin production via tyrosinase inhibition (Figure 4) provides insight into the potential mechanism of action for how GSE affects skin pigmentation. Filaggrin is critical for epidermal barrier function and a previous report showed that a decrease in PP2A activity impaired filaggrin processing [9]. Thus, we can speculate that E-AGSE's ability to activate PP2A is what allows it to boost filaggrin levels, which are reduced when skin is irradiated with UVB (Figure 1). In addition to promoting barrier function, E-AGSE when applied topically also protected against UVB-induced DNA damage and inflammation, reducing the presence of cyclobutene pyrimidine dimers (CPDs), sunburn cells (SBCs), and the release of IL-8 (Figure 3 and Table 4) in vitro. It has been previously reported that PP2A is a key regulator of NF-κB-induced inflammation and apoptosis where UVB mediates the inactivation of PP2A, leading to cell death and pro-inflammatory cytokine production [44]. The DEJ plays a vital role in barrier repair, hydration, and skin aging. The DEJ and its components tightly connect the epidermis to the fibrous structure of the dermis, which effectively keeps skin firm yet elastic, while also functioning as a transport channel for moisture and nutrients required by the epidermis. Skin aging can negatively alter the DEJ, and our results demonstrate that E-AGSE significantly increased the gene expression of important DEJ markers including OCLN, SDC1, HSPG2, and CD44. The results presented here lend further support to the hypothesis that agents that promote PP2A function, such as AGSE and E-AGSE, can boost skin health by protecting against several deleterious effects caused by extended exposure to UV light. We are excited to report here both in vitro and human clinical activity for E-AGSE. Much effort is still required to fully understand the role PP2A plays in oxidative stress, aging, and skin health, but we look forward to continuing to elucidate the mechanisms of action for this emerging new target in skin.

5. Conclusions

We demonstrate here for the first time E-AGSE as a multifunctional ingredient for combating skin aging and promoting a youthful appearance. The E-AGSE formulation was created using liposomes and micelles, resulting in a more soluble, lighter-colored formulation and making it more suitable for use in a wider range of skincare products. E-AGSE not only promotes the production of collagens, elastin, filaggrin, and DEJ markers, but can also protect skin against UVB-induced inflammation and DNA damage. Additionally, E-AGSE showed activity in skin-brightening endpoints, reducing melanin production

in melanocytes and inhibiting tyrosinase activity. Clinical results showed that E-AGSE's in vitro activity translates to human subjects, with 2% E-AGSE Essence applied topically being well tolerated and effective in reducing the appearance of wrinkles and improving skin brightness and hydration in human subjects. Our next goals are to investigate the transdermal absorption profile of E-AGSE compared to AGSE, and increase the availability of the formulation to be tested and evaluated.

Supplementary Materials: The following are available online at https://www.mdpi.com/article/10.3390/cosmetics9010004/s1, Figure S1: E-AGSE aqueous solutions after 3 months at various temperatures, Figure S2: Arbutin control in tyrosinase enzyme activity assay, Figure S3: Cell viability of test materials in culture, Table S1: Clinical study demographics.

Author Contributions: Conceptualization, K.T., L.G., X.H., E.P. and J.R.F.; methodology, J.R.F. and J.H.; software, J.R.F. and J.H.; validation, J.R.F. and E.P.; formal analysis, K.T., L.G., X.H., M.T., J.R.F. and E.P.; investigation, K.T., L.G., X.H., J.R.F., M.T. and E.P.; resources, K.T., L.G., X.H., J.R.F., E.P., C.F.; data curation, K.T., L.G., X.H., J.R.F. and E.P.; writing—original draft preparation, J.R.F. and E.P.; writing—review and editing, K.T., L.G., X.H., J.R.F., C.F., K.R., J.H., E.P.; visualization, J.R.F.; supervision, K.T., L.G., X.H., M.S., J.B.S. and E.P.; project administration, K.T., L.G., X.H., J.R.F., M.S., J.B.S. and E.P.; funding acquisition, K.T. and E.P. All authors have read and agreed to the published version of the manuscript.

Funding: This research received no external funding.

Institutional Review Board Statement: The study was conducted according to the guidelines of the Declaration of Helsinki and approved by the Institutional Review Board of SGS Stephens (No. SHCPCH210201806 and approved in January 2021).

Informed Consent Statement: Informed consent was obtained from all subjects involved in the study.

Data Availability Statement: Data available upon request to corresponding author: jfernandez@signumbio.com.

Conflicts of Interest: K.T., L.G. and X.H. are employees of Shanghai Chicmax Cosmetic Co., Ltd., K.R., M.T., J.H., C.F., M.S., E.P. and J.R.F. are employees of Signum Biosciences, Inc., J.B.S. serves on the board of directors. All authors have stock and/or stock options in the company.

References

1. Rabe, J.H.; Mamelak, A.J.; McElgunn, P.J.; Morison, W.L.; Sauder, D.N. Photoaging: Mechanisms and repair. *J. Am. Acad. Dermatol.* **2006**, *55*, 1–19. [CrossRef] [PubMed]
2. Pinnell, S.R. Cutaneous photodamage, oxidative stress, and topical antioxidant protection. *J. Am. Acad. Dermatol.* **2003**, *48*, 1–22. [CrossRef] [PubMed]
3. Farage, M.A.; Miller, K.W.; Elsner, P.; Maibach, H.I. Intrinsic and extrinsic factors in skin ageing: A review. *Int. J. Cosmet. Sci.* **2008**, *30*, 87–95. [CrossRef] [PubMed]
4. Yamaguchi, Y.; Brenner, M.; Hearing, V.J. The Regulation of Skin Pigmentation. *J. Biol. Chem.* **2007**, *282*, 27557–27561. [CrossRef] [PubMed]
5. Koh, E.M.; Lee, E.K.; Song, C.H.; Song, J.; Chung, H.Y.; Chae, C.H.; Jung, K.J. Ferulate, an Active Component of Wheat Germ, Ameliorates Oxidative Stress-Induced PTK/PTP Imbalance and PP2A Inactivation. *Toxicol. Res.* **2018**, *34*, 333–341. [CrossRef] [PubMed]
6. Li, S.; Mhamdi, A.; Trotta, A.; Kangasjarvi, S.; Noctor, G. The protein phosphatase subunit PP2A-B'gamma is required to suppress day length-dependent pathogenesis responses triggered by intracellular oxidative stress. *New Phytol.* **2014**, *202*, 145–160. [CrossRef]
7. Elgenaidi, I.S.; Spiers, J.P. Regulation of the phosphoprotein phosphatase 2A system and its modulation during oxidative stress: A potential therapeutic target? *Pharmacol. Ther.* **2019**, *198*, 68–89. [CrossRef]
8. O'Shaughnessy, R.F.; Welti, J.C.; Sully, K.; Byrne, C. Akt-dependent Pp2a activity is required for epidermal barrier formation during late embryonic development. *Development* **2009**, *136*, 3423–3431. [CrossRef]
9. Kam, E.; Nirunsuksiri, W.; Hager, B.; Fleckman, P.; Dale, B.A. Protein phosphatase activity in human keratinocytes cultured from normal epidermis and epidermis from patients with harlequin ichthyosis. *Br. J. Dermatol.* **1997**, *137*, 874–882. [CrossRef]
10. Dobrowsky, R.T.; Kamibayashi, C.; Mumby, M.C.; Hannun, Y.A. Ceramide activates heterotrimeric protein phosphatase 2A. *J. Biol. Chem.* **1993**, *268*, 15523–15530. [CrossRef]
11. Voronkov, M.; Braithwaite, S.P.; Stock, J.B. Phosphoprotein phosphatase 2A: A novel druggable target for Alzheimer's disease. *Future Med. Chem.* **2011**, *3*, 821–833. [CrossRef]

12. Jeong, H.S.; Yun, H.Y.; Baek, K.J.; Kwon, N.S.; Park, K.C.; Kim, D.S. Okadaic acid suppresses melanogenesis via proteasomal degradation of tyrosinase. *Biol. Pharm. Bull.* **2013**, *36*, 1503–1508. [CrossRef]

13. Weseler, A.R.; Bast, A. Masquelier's grape seed extract: From basic flavonoid research to a well-characterized food supplement with health benefits. *Nutr. J.* **2017**, *16*, 5. [CrossRef] [PubMed]

14. Yamakoshi, J.; Otsuka, F.; Sano, A.; Tokutake, S.; Saito, M.; Kikuchi, M.; Kubota, Y. Lightening effect on ultraviolet-induced pigmentation of guinea pig skin by oral administration of a proanthocyanidin-rich extract from grape seeds. *Pigment Cell Res.* **2003**, *16*, 629–638. [CrossRef] [PubMed]

15. Cronin, H.; Draelos, Z.D. Original Contribution: Top 10 botanical ingredients in 2010 anti-aging creams. *J. Cosmet. Dermatol.* **2010**, *9*, 218–225. [CrossRef] [PubMed]

16. Zillich, O.V.; Schweiggert-Weisz, U.; Eisner, P.; Kerscher, M. Polyphenols as active ingredients for cosmetic products. *Int. J. Cosmet. Sci.* **2015**, *37*, 455–464. [CrossRef] [PubMed]

17. Huber, K.L.; Fernández, J.R.; Webb, C.; Rouzard, K.; Healy, J.; Tamura, M.; Stock, J.B.; Stock, M.; Pérez, E. AGSE: A Novel Grape Seed Extract Enriched for PP2A Activating Flavonoids That Combats Oxidative Stress and Promotes Skin Health. *Mol.* **2021**, *26*, 6351. [CrossRef] [PubMed]

18. Fernandez, J.R.; Huber, K.L.; Webb, C.; Rouzard, K.; Tamura, M.; Wang, Y.; Liao, Z.; Sun, P.; Nie, J.; Zhang, Z.; et al. TIRACLE™ and ACTIVITIS™: A novel anti-aging blend. *J. Investig. Dermatol.* **2019**, *139*, PB17. [CrossRef]

19. Lohani, A.; Verma, A.; Joshi, H.; Yadav, N.; Karki, N. Nanotechnology-Based Cosmeceuticals. *ISRN Dermatol.* **2014**, *2014*, 1–14. [CrossRef]

20. Zhou, H.; Luo, D.; Chen, D.; Tan, X.; Bai, X.; Liu, Z.; Yang, X.; Liu, W. Current Advances of Nanocarrier Technology-Based Active Cosmetic Ingredients for Beauty Applications. *Clin. Cosmet. Investig. Dermatol.* **2021**, *14*, 867–887. [CrossRef]

21. Schlupp, P.; Blaschke, T.; Kramer, K.; Höltje, H.-D.; Mehnert, W.; Schäfer-Korting, M. Drug Release and Skin Penetration from Solid Lipid Nanoparticles and a Base Cream: A Systematic Approach from a Comparison of Three Glucocorticoids. *Ski. Pharmacol. Physiol.* **2011**, *24*, 199–209. [CrossRef] [PubMed]

22. Abramovits, W.; Granowski, P.; Arrazola, P. Applications of nanomedicine in dermatology: Use of nanoparticles in various therapies and imaging. *J. Cosmet. Dermatol.* **2010**, *9*, 154–159. [CrossRef] [PubMed]

23. Ganceviciene, R.; Liakou, A.I.; Theodoridis, A.; Makrantonaki, E.; Zouboulis, C.C. Skin anti-aging strategies. *Dermato-Endocrinology* **2012**, *4*, 308–319. [CrossRef] [PubMed]

24. Uitto, J. The role of elastin and collagen in cutaneous aging: Intrinsic aging versus photoexposure. *J. Drugs Dermatol.* **2008**, *7*, 12–16.

25. Schagen, S.K. Topical Peptide Treatments with Effective Anti-Aging Results. *Cosmetics* **2017**, *4*, 16. [CrossRef]

26. Vázquez, F.; Palacios, S.; Alemañ, N.; Guerrero, F. Changes of the basement membrane and type IV collagen in human skin during aging. *Maturitas* **1996**, *25*, 209–215. [CrossRef]

27. Roig-Rosello, E.; Rousselle, P. The Human Epidermal Basement Membrane: A Shaped and Cell Instructive Platform That Aging Slowly Alters. *Biomolecules* **2020**, *10*, 1607. [CrossRef]

28. Gallo, R. Proteoglycans and glycosaminoglycans of skin. *Dermatol. Gen. Med.* **1999**, *1*, 283–288.

29. Pummi, K.; Malminen, M.; Aho, H.; Karvonen, S.-L.; Peltonen, J.; Peltonen, S. Epidermal Tight Junctions: ZO-1 and Occludin are Expressed in Mature, Developing, and Affected Skin and In Vitro Differentiating Keratinocytes. *J. Investig. Dermatol.* **2001**, *117*, 1050–1058. [CrossRef]

30. Pineau, N.; Bernerd, F.; Cavezza, A.; Dalko-Csiba, M.; Breton, L. A new C-xylopyranoside derivative induces skin expression of glycosaminoglycans and heparan sulphate proteoglycans. *Eur. J. Dermatol.* **2008**, *18*, 36–40.

31. Pageon, H.; Azouaoui, A.; Zucchi, H.; Rocois, S.; Tran, C.; Asselineaau, D. Potentially beneficial effects of rhamnose on skin ageing: An in vitro and in vivo study. *Int. J. Cosmet. Sci.* **2019**, *41*, 213–220. [CrossRef]

32. Wegrowski, Y.; Maquart, F.; Borel, J. Stimulation of sulfated glycosaminoglycan synthesis by the tripeptide-copper complex Glycyl-L-histidyl-L-lysine-Cu2+. *Life Sci.* **1992**, *51*, 1049–1056. [CrossRef]

33. Strickland, I.; Rhodes, L.E.; Flanagan, B.F.; Friedmann, P.S. TNF-α and IL-8 Are Upregulated in the Epidermis of Normal Human Skin after UVB Exposure: Correlation with Neutrophil Accumulation and E-Selectin Expression. *J. Investig. Dermatol.* **1997**, *108*, 763–768. [CrossRef] [PubMed]

34. Mildner, M.; Jin, J.; Eckhart, L.; Kezic, S.; Gruber, F.; Barresi, C.; Stremnitzer, C.; Buchberger, M.; Mlitz, V.; Ballaun, C.; et al. Knockdown of Filaggrin Impairs Diffusion Barrier Function and Increases UV Sensitivity in a Human Skin Model. *J. Investig. Dermatol.* **2010**, *130*, 2286–2294. [CrossRef] [PubMed]

35. Cadet, J.; Douki, T. Formation of UV-induced DNA damage contributing to skin cancer development. *Photochem. Photobiol. Sci.* **2018**, *17*, 1816–1841. [CrossRef] [PubMed]

36. McDaniel, D.H.; Neudecker, B.A.; DiNardo, J.C.; Lewis, J.A.; Maibach, H.I. Idebenone: A new antioxidant—Part, I. Relative assessment of oxidative stress protection capacity compared to commonly known antioxidants. *J. Cosmet. Dermatol.* **2005**, *4*, 10–17. [CrossRef]

37. Sharif, A.; Akhtar, N.; Khan, M.S.; Menaa, A.; Menaa, B.; Khan, B.A.; Menaa, F. Formulation and evaluation on human skin of a water-in-oil emulsion containing Muscat hamburg black grape seed extract. *Int. J. Cosmet. Sci.* **2014**, *37*, 253–258. [CrossRef]

38. Iozumi, K.; Hoganson, G.E.; Pennella, R.; Everett, M.A.; Fuller, B.B. Role of Tyrosinase as the Determinant of Pigmentation in Cultured Human Melanocytes. *J. Investig. Dermatol.* **1993**, *100*, 806–811. [CrossRef]

39. Otto, A.; Du Plessis, J.; Wiechers, J.W. Formulation effects of topical emulsions on transdermal and dermal delivery. *Int. J. Cosmet. Sci.* **2009**, *31*, 1–19. [CrossRef]

40. Hemmati, A.A.; Foroozan, M.; Houshmand, G.; Moosavi, Z.B.; Bahadoram, M.; Maram, N.S. The Topical Effect of Grape Seed Extract 2% Cream on Surgery Wound Healing. *Glob. J. Health Sci.* **2014**, *7*, 52–58. [CrossRef]

41. Giacomelli, L.; Togni, S.; Meneghin, M.; Eggenhooffner, R.; Maramaldi, G. In vivo validation of the multicomponent powder (Vitachelox(R)) against the deposition of polluting ions. *Clin. Cosmet. Investig. Dermatol.* **2018**, *11*, 109–113. [CrossRef] [PubMed]

42. Kapoor, S.; Saraf, S. Assessment of viscoelasticity and hydration effect of herbal moisturizers using bioengineering techniques. *Pharmacogn. Mag.* **2010**, *6*, 298–304. [CrossRef] [PubMed]

43. Grether-Beck, S.; Marini, A.; Jaenicke, T.; Krutmann, J. Effective photoprotection of human skin against infrared A radiation by topically applied antioxidants: Results from a vehicle controlled, double-blind, randomized study. *Photochem. Photobiol.* **2015**, *91*, 248–250. [CrossRef] [PubMed]

44. Barisic, S.; Strozyk, E.; Peters, N.; Walczak, H.; Kulms, D. Identification of PP2A as a crucial regulator of the NF-kappaB feedback loop: Its inhibition by UVB turns NF-kappaB into a pro-apoptotic factor. *Cell. Death Differ.* **2008**, *15*, 1681–1690. [CrossRef] [PubMed]